A modified sol-gel method using acetone-ethanol mixed solvent for fast constructing nanometric TiO_2 shells

Author name: Wanghui Chen, Chika Takai, Hadi Razavi Khosroshahi, Masayoshi Fuji*, Takashi Shirai

Author affiliation: Advanced Ceramics Research Center, Nagoya Institute of Technology, Honmachi 3-101-1, Tajimi, Gifu, 507-0033, Japan

*Corresponding author: E-mail: fuji@nitech.ac.jp; Tel.: +81 572 24 8110; Fax: +81 572 24 8109.

Abstract: We successfully constructed uniform and complete TiO_2 shells on SiO_2 cores in a short reaction time (2h) and obtained the core-shell particles with high dispersibility. In this modified sol-gel method, the adopting of ethanol-acetone mixed solvent was critical and advantageous for the fast formation of TiO_2 shells. When acetone was controlled at an optimum fraction in solvent (acetone: ethanol=1.2:1 v/v), it not only increased the hydrolysis rate of precursor (i. e., titanium (IV) tetrabutoxide) and the condensation rate of titanium oligomers, but also regulated these two sub-reactions of TiO_2 formation to be in balance ─ and thus suppressed the occurrence of agglomeration during TiO_2 coating. In addition, the influence of the concentration of catalyst NH_3 and precursor titanium (IV) tetrabutoxide was also investigated. Furthermore, the thickness of TiO_2 shells on 366nm SiO_2 cores was varied from 30 to 107 nm by simply adjust the addition volume of precursor, as the regulation role of acetone was widely applicable for different concentration of precursor. Finally, the obtained TiO_2 shells were proved to be able to crystallize to anatase shells by calcination, while the core-shell structure showed high stability at high temperature.

Keywords: Core-shell; D. TiO_2; D. Glass; A. Sol-gel processes.

1

Introduction

In the past several years, ceramic core-shell particles (including x@ceramic, ceramic@x and ceramic@ceramic; x=polymer, metal, carbon, etc.) have received significant research attention, because of their potential applications in energy conversion, heterogeneous catalysis, drug delivery, bio-compatible material, thermal insulation, etc [1-10]. The competitiveness of this class of composite particles comes from their novel hetero-structure, which combines two or more materials in one unit—and thus brings the multifunctionality and synergistic effect [11-13]. To date, a number of synthetic strategies have been developed for ceramic core-shell particles, such as sol-gel method [14-17], layer-by-layer approach [18], hydrothermal reaction [19, 20], etc. Among them, sol-gel method was commonly adopted for constructing most kinds of ceramic shells, in the advantages of its short production cycle and feasibility under moderate condition. Representatively, SiO_2 shell was constructed on various kinds of core materials, including polymers, metals and ceramics, by conducting the hydrolysis of tetraethyl orthosilicate (TEOS) and related condensation in core suspensions, with the catalyzing of NH_3 [21].

There is no doubt the performance of ceramic core-shell particles in applications is closely related to their dispersibility, as well as the uniformity and completeness of their shells. Concerning these points, to the best of our knowledge, it remains a great challenge for constructing uniform TiO_2 shells and obtaining the core@TiO_2 particles with high dispersibility by the conventional sol-gel process, as conducting the hydrolysis reaction of titanium alkoxides and related condensations in ethanol with the presence of ammonia. Different with that for SiO_2 shells, the concentration of titanium oligomers in the reaction solution could hardly be controlled on an appropriate level for heterogeneous nucleation, due to the ultra-high hydrolysis

speed of their precursors (i. e., titanium alkioxides). Instead, there were a certain number of freestanding TiO_2 particles generated in bulk solution by homogeneous nucleation, and subsequently reduced the yield rate of TiO_2 coating. Even worse, those TiO_2 particles would possibly form necks between core-shell particles, and then caused particle agglomeration. Although Wei Li et al [22] most recently reported the concentration of titanium oligomers could be well controlled on an appropriate level for the heterogeneous nucleation by precisely adjusting the concentration of NH_3 (played as the catalyst) to a low level, such a low concentration of NH_3 also led to a low yielding rate of TiO_2. Therefore, a long reaction time and certain heating were required in their synthesis. Meanwhile, the thickness of TiO2 shells in that work could only be tuned by varying the yield rate of TiO_2, which was not as advantageous as by adjusting the amount of precursor on the basis of a high yield rate of TiO_2.

Herein, we introduce a modified sol-gel method to fast constructing uniform TiO_2 shells and fabricate core@TiO_2 particles with high dispersibility. The key point of this method is adding acetone, which is known as a cheap and commonly used chemical, into the conventional reaction solution of ethanol/NH_3/water/TBOT and controlling it in an appropriate fraction. For easily analyzing the formation of TiO_2 shells and measuring the shell thickness, monodisperse SiO_2 microspheres were chosen as the core material. Meanwhile, a commonly used titanium alkioxide—titanium (IV) tetrabutoxide (TBOT) was used as the precursor of TiO_2. The obtained SiO_2@TiO_2 core-shell particles (STcsps) showed high dispersibility and were found uniform in shell thickness. In contribution of the role of acetone, it was also possible to tuning the TiO_2 shell thickness by the concentration of TBOT in reaction solution. It is also noteworthy that surfactants were unnecessary in this method and the reaction could be finished in a short time with reaching to a high yield rate of TiO_2 coating.

2. Experimental

2.1 Materials

Tetraethyl orthosilicate (TEOS, 95.0%), Ethanol (99.5%), Ammonia solution (28.0 %), Titanium (IV) Tetrabutoxide (TBOT, 95.0%), Acetone (99.5%) were from Wako Pure Chemical Industries, Ltd. (Japan). All the chemicals were used as received and without further purification. DI water was produced by RFD250NB distilled water system (Toyo Roshi Kaisha, Ltd., Japan).

2.2 Synthesis of SiO_2 cores

SiO_2 cores were synthesized by the Stöber method using TEOS as the precursor and NH_3 as the catalyst [23]. Briefly, 10ml 28.0% ammonia solution was added into a mixture of 36ml ethanol and 20ml DI water under vigorous stirring (600rpm). After 20min, 35.6 ml TEOS solution (15.7 vol. % in ethanol) was poured into the above mixture to initiate the sol-gel process for SiO_2. After 8h, resulting particles were collected by centrifugation at 3000rpm (using H-9R, Kokusan co. Ltd. Japan) and washed with ethanol and DI water for several times. These particles were finally dried in vacuum at 80°C for 12h.

2.3 Fabrication of STcsps

Reaction solution for the fabrication STcsps contained ethanol, acetone, NH_3, water, TBOT, and SiO_2 cores. All the recipes for these fabrications are listed in **Table 1**. In a typical process (recipe 4), an amount of 0.025g SiO_2 cores was dispersed in a mixture of acetone (28.50ml), ethanol (16.50ml) and ammonia solution (28.0%, 0.15ml). Then the suspension was treated by ultrasound for 30min to improve its uniformity. After that, 5ml TBOT solution (2.0 vol. % in ethanol) was poured in under vigorous stirring (600rpm). Then the reaction lasted for 2h at

room temperature with the same stirring. Productions were collected by centrifugation at

3000rpm (using H-9R, Kokusan co. Ltd., Japan) and then washed with ethanol and DI water

for 6 times in sequence. Finally, the production was dried in vacuum at $80^{\circ}C$ for 12h.

Calcinations of STcsps were carried out in air at 500, 550 and $600^{\circ}C$, respectively. All the

calcinations lasted for 5h and with the heating rate of $5^{\circ}C/min$.

2.4 Characterization

Scan electron microscopy (SEM) images were taken by a JSM-7600F (JEOL Ltd., Japan).

Transmission electron microscopy (TEM) images and Energy dispersive X-ray spectroscopy

(EDS) mapping were taken by a JEM-z2500 (JEOL Ltd., Japan). Thermogravimetry (TG-DTA)

curves were recorded by a thermo plus TG-8120 (Rigaku. Co., Japan). X-ray diffraction patterns

were recorded by a Ultima IV (Rigaku co., Japan) with Cu Kα radiation (λ=1.5418 Å). Dynamic

Light Scattering (DLS) measurements were conducted on a Zetasizer nano-zs (Malvern Ltd.,

UK) for analyzing particle size distribution. FT-IR spectra were retrieved from a FT/IR-6000

(Jasco Co., Ltd., Japan).

3. Result and discussion

3.1 Formation of TiO_2 shells with the presence of acetone

The as-synthesized SiO_2 microspheres (i. e., cores for TiO_2 coating) showed uniform size

and good dispersibility in their SEM image (**Figure 1a**). The mean size of SiO_2 cores was

calculated to 366±3nm by evaluating 100 particles in SEM image (magnification: 20,000).

Meanwhile, the size distribution curve of SiO_2 cores (in **Figure 1h**), with the polydispersity

index (PDI) as low as 0.012, further indicates their high monodispersibility.

Figure 1b~g demonstrate a typical formation process of STcsps in the adopted reaction solution of ethanol/acetone/NH$_3$/water/TBOT (**recipe 4**). The intermediate productions for SEM observations were collected at 2, 10, 20, 40, 60 and 120min, respectively. As seen, TiO$_2$ started to deposit on the surface of SiO$_2$ cores soon after the initiation of TiO$_2$ coating reaction (2min), with leading to a much rougher particle surface. After reacting for 10min, the surface of SiO$_2$ cores was completely covered by immobilized TiO$_2$ particles. Then the particle size rapidly increased and reached to a stable stage after 1h. In the end of the reaction, the mean size of produced STcsps was calculated to 536±5nm, much larger than that of the corresponding SiO$_2$ cores. Moreover, it was clear that the high monodispersibility of SiO$_2$ cores was maintained well in the course of size increasing, indicating the uniformity of TiO$_2$ shells. Meanwhile, the absence of freestanding TiO$_2$ particles implied the high yield of TiO$_2$ coating (the free TiO$_2$ nanoparticles in **Figure 1b** were possibly caused by the ultrasound treatment during sampling). Agglomeration was also well suppressed in this course, as there is only one peak appeared between 100 and 10000nm in the size distribution curve of every intermediate production (**Figure 1h**). It should be point out that although the mean size of STcsps only showed a slight increasing after 1h, as indicated by both SEM observations and DLS measurements, an appropriate extension on the reaction time was necessary in practical operations for the aging of TiO$_2$.

Core-shell structure of the obtained STcsps was further confirmed by TEM observation. Since TiO$_2$ and SiO$_2$ show different contrast under electron beam, one can easily distinguish the shell and core parts of STcsps in the dark-field TEM image. As seen in **Figure 2a**, a complete and uniform TiO$_2$ shell formed on the surface of every SiO$_2$ core. Meanwhile, the interface between TiO$_2$ shell and SiO$_2$ core could be observed in the high-magnification TEM image

(**Figure 2b**). It's also found the formed TiO_2 shells were composed by numerous closely-staking TiO_2 particles. EDS mapping is also an intuitive evidence for the core-shell structure of STcsps, as seen in **Figure 2c**, Ti element (**c1**) accumulated near the edge of STcsps while Si element (**c2**) was rich in the interior of particle. O element (**c3**) uniformly distributed in the whole STcsps, because of the similar chemical formula between SiO_2 and TiO_2. Other evidences for the composition of SiO_2 and TiO_2, such as EDS point spectra and FT-IR spectra, were given in the supplementary material (**s1~s3**).

3.2 The role of acetone

On the basis of above observations, STcsps with high dispersiblity and uniform shells could be successfully obtained when the volume ratio of acetone to ethanol ($R_{a/e}$) was controlled at 1.2 (**Figure 1g**). To analyze the influence of acetone, other batches of STcsps were fabricated with controlling $R_{a/e}$ at 0, 0.4, 0.8, 1.6 and 2.0, respectively. In brief, the yield rate of TiO_2 coating increased with increasing $R_{a/e}$, while particle agglomeration occurred when $R_{a/e}$ was excessively high. When low $R_{a/e}$ (≤ 0.4) was adopted (**Figure 3a**), there was no TiO_2 yielded within the specified reaction time (2h), indicating the low hydrolysis rate of TBOT under this condition. When $R_{a/e}$ reached to 0.80 (**Figure 3b**), flocculent TiO_2 generated and adhered on the surface of cores, though their amount was far from enough to form complete shells. The amount of yielded TiO_2 significantly increased when $R_{a/e}$ was further increased to 1.2 (**Figure 1g**), and thus immobilized TiO_2 particles were able to form uniform and complete shells. However, when $R_{a/e}$ was increased to 1.6, necks and freestanding TiO_2 particles appeared accompanying with the formation of TiO_2 shells (**Figure 3c**), and correspondingly, the high dispersibility of STcsps could not be maintained any longer. If $R_{a/e}$ was controlled at 2.00 or
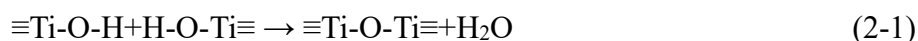
1   even higher, only irregular aggregates could be found in the production (**Figure 3d**).

2   As we know, the sol-gel process from TBOT to TiO_2 can be described by following two

3   sub-reactions [24]:

4   (i) Hydrolysis of TBOT ($R=C_4H_9$),

$$\equiv\text{Ti-O-R}+H_2O \rightarrow \equiv\text{Ti-O-H}+ ROH \qquad (1\text{-}1)$$

5   (ii) Condensation of titanium oligomers

$$\equiv\text{Ti-O-H}+\text{H-O-Ti}\equiv \rightarrow \equiv\text{Ti-O-Ti}\equiv+H_2O \qquad (2\text{-}1)$$

6   or

$$\equiv\text{Ti-O-H}+\text{R-O-Ti}\equiv \rightarrow \equiv\text{Ti-O-Ti}\equiv+ROH \qquad (2\text{-}2)$$

7   According to LaMer theory [25], the concentration of titanium oligomers (C_{to}) in reaction

8   solution determined whether TiO_2 would form or not. In general, C_{to} first increased along with

9   the hydrolysis of TBOT and condensation of titanium monomers until it reached to a critical

10   concentration. Once a sufficient number of titanium oligomers containing certain numbers of

11   structure units (i. e., -O-Ti-O-) had been yielded, polymerized TiO_2 networks (i. e.,

12   polyoxoalcoxides) formed along with further condensations, followed by the precipitation of

13   TiO_2 from bulk solution(TiO_2 nuclei) [24]. Apparently, the condensation process in this stage

14   could be seen as the consumption of titanium oligomers, and its rate determined if the C_{to} in

15   reaction solution would continuously increase or not. Moreover, the nucleation type of TiO_2

16   was also determined C_{to}, as if it was only exceeded the critical concentration for heterogeneous

17   nucleation (C_{he}) or even exceeded that for homogeneous nucleation (C_{ho}). In the latter case,

18   TiO_2 nuclei formed by both heterogeneous and homogeneous nucleation. Obviously, for

19   obtaining the TiO_2-coated particles with desirable morphology: (i) the hydrolysis rate should be

20   high enough to yield sufficient amount of titanium oligomers for initiating the nucleation of

8

TiO$_2$; (ii) the condensation rate of titanium oligomers should be high enough to ensure C$_{to}$ would not exceed C$_{ho}$.

In this work, it is clear the hydrolysis of TBOT was accelerated by the addition of acetone, and thus C$_{to}$ was sufficiently high to initiate the nucleation event of TiO$_2$, though there was only a small fraction of NH$_3$ catalyst contained in the reaction solution. When R$_{a/e}$=1.2, the heterogeneous nucleation was maintained for a considerable long period to yield a sufficient number of TiO$_2$ nuclei for complete coating, whereas homogeneous nucleation and its related agglomeration were well suppressed. Obviously, C$_{to}$ in this case was lower than C$_{ho}$ but higher than C$_{he}$. Therefore, it is rational that the condensation process of titanium oligomers was also promoted by acetone —only then could it be in balance with the accelerated TBOT hydrolysis and to maintain the appropriate level of C$_{to}$. However, it seems the balance no longer existed with further increasing R$_{a/e}$ to 1.6 or higher, as indicated by the freestanding TiO$_2$ particles and agglomeration. In this case, since the kinetic rate of both the hydrolysis rate of TBOT and the condensation rate of titanium oligomers had been greatly enhanced by such a high fraction of acetone, the two sub-reactions of TiO$_2$ formation possibly became diffusion-controlled. Obviously, since the condensation reaction (eq. 2-1 or 2-2) involves the mass diffusion of two titanium oligomers, its apparent rate is much lower than that of the hydrolysis reaction. Therefore, C$_{to}$ would keep increasing after it exceeded C$_{he}$, and followed by exceeding C$_{ho}$ to initiate the homogeneous nucleation of TiO$_2$. It should be point out if acetone was absent in the reaction solution, STcsps with uniform TiO$_2$ shells and high dispersibility might also be obtained by precisely controlling the fraction of ammonia [22]. Nevertheless, it seems the hydrolysis rate of TBOT and condensation rate of titanium oligomers could only balance with each other when both of them were low. Therefore, the production cycle would be much longer

1   than that adopted in this work (2h).

2   The mechanism of acetone promoting both the hydrolysis of TBOT and the condensation

3   of titanium oligomers could be classified to an issue on solvent effect. As we know, both of the

4   hydrolysis reaction of TBOT and the condensation of titanium oligomers under base condition

5   are nucleophilic substitution reactions. However, as a protic solvent, ethanol would possibly

6   hydrogen bond with hydroxyl ions (i. e., catalysts) in hydrolysis reaction and with nucleophilic

7   deprotonated silanols in condensation reaction, and thus retard the processing rate of these two

8   nucleophilic substitution reactions. Apparently, the presence of acetone, as a typical aprotic

9   solvent, weakened the hydrogen bond between reactive species and ethanol —the rate of TBOT

10   hydrolysis and titanium oligomers condensation were therefore increased. Furthermore, on the

11   increasing of condensation rate, the polarity of solvent should also be taken into consideration.

12   Since the dielectric constant of acetone (21.0) is lower than that of ethanol (24.5), the solvation

13   effect of generated titanium oligomers (or monomers) was weakened after the appearance of

14   acetone. In other words, titanium oligomers (or monomers) in ethanol-acetone mixture were

15   not as "solvable" as that in ethanol. Therefore, they were more likely to conduct condensation

16   and then precipitate from liquid phase. Last but not the least, the addition of acetone also

17   reduced the viscosity of the reaction solution, as the viscosity of acetone (3.06×10^{-4} pa·s) is

18   about one-third to that of ethanol (1.074×10^{-3} pa·s). Since a low viscosity is obviously

19   advantageous for the mass transference of reactive species, the reduction of viscosity could also

20   be seen one of rational reasons for the promoting of both the hydrolysis of TBOT and the

21   condensation of titanium oligomers.

22   Although there still need much more experiments to analyze its actual mechanism, the

23   regulation role of the regulation role of acetone towards the formation of TiO_2 has also been

10

proved by synthesizing monodisperse TiO_2 microspheres (**s4**). To our knowledge, monodisperse TiO_2 microspheres could hardly be synthesized by conventional sol-gel method with only using ethanol as the solvent, since the hydrolysis rate of TBOT in that case was always higher than the condensation rate of titanium oligomers [26].

3.3 Effect of NH_3

Figure 4a shows the SEM image of STcsps fabricated without the presence of NH_3 in reaction solution (**recipe 7**). For this fabrication, all parameters were kept the same with **recipe 4** except replacing the added 0.15ml 28.0% ammonia solution with 0.11ml DI water for excluding NH_3 but maintaining the concentration of water in reaction solution. The morphology of STcsps formed under this condition was unfavorable, as there were a number of necks formed between particles. Even worse, the surface of SiO_2 cores was not completely covered. Instead, immobilized TiO_2 particles only formed a loose and porous layer on every SiO_2 core. To explain this phenomenon, the repulsive force between SiO_2 cores and titanium oligomers should be taken into consideration. If NH_3 was absent in reaction solution, since both the SiO_2 cores and titanium oligomers carried negative charges, it was hard for titanium oligomers overcoming the energetic barrier to conduct heterogeneous nucleation. Instead, freestanding TiO_2 particles would be yielded in the bulk solution due to the ongoing increasing of C_{to}. On contrary, when a certain amount of NH_3 was added in, energetic barrier for the heterogeneous nucleation of TiO_2 was reduced by the absorbed NH_4^+ ions on the surface of SiO_2 cores. Therefore, the yield and uniformity of TiO_2 coating was improved.

Although the presence of NH_3 in the reaction solution is a prerequisite for achieving a successful TiO_2 coating, the morphology of STcsps was sensitive to addition volume of

11

ammonia solution—severe agglomeration occurred even when the addition volume of ammonia solution was slightly increased to 0.25ml (**Figure 4b**). This result showed good agreement with that of previous works [22], and could be attributed to the excessively high hydrolysis rate of TBOT at high pH. Apparently, the formation rate of TiO_2 in the reaction solution of ethanol/acetone/NH_3/water/TBOT was determined by both $R_{a/e}$ (i. e., fraction of acetone) and the concentration of NH_3. There might still be an optimum $R_{a/e}$ with such a high concentration of NH_3, but to find this optimum $R_{a/e}$ is already out of the scope of this paper. Nevertheless, it should be point out that regulating the TiO_2 formation by $R_{a/e}$ is much more convenience and practical than that by controlling the concentration of NH_3 in reaction solution, because of the small usage volume and high volatility of ammonia solution.

3. 4 Constructing TiO_2 shells with various thickness

Figure 1g and **5a~e** show SEM images STcsps fabricated with different concentration of TBOT (C_{TBOT}) while fixing $R_{a/e}$ at 1.2 and the addition volume of ammonia solution at 0.15ml. The size information of all these STcsps were calculated by evaluating 100 particles in SEM images (magnification: 20,000) and listed following their corresponding recipes (**4, 9~13**) in **Table 1**. As seen, the average size of STcsps could be varied from 426 to 692nm by varying C_{TBOT} from 0.2 to 1.0 vol. %, indicating TiO_2 shells with different thickness had been constructed on SiO_2 cores. Moreover, the obtained STcsps showed high dispersibility when C_{TBOT} was controlled lower than 0.75 vol. %, whereas some necks formed when C_{TBOT} reached to 1.00 vol. % (**Figure 5e**).

The thickness of TiO_2 shell (T/nm) was calculated by the following equation:

$$T = \left(d_{STcsps} - d_{cores}\right)/2 \qquad (3)$$

1 Mean while, the thickness of TiO_2 shells were also calculated theoretically (i. e., T_{theo}/nm) by

2 the following equations with assuming the conversion rate of TBOT reached to100%:

$$2T_{theo} = d_{cores} \cdot \sqrt[3]{\left(m_{TiO_2}/\rho_{TiO_2} + m_{SiO_2}/\rho_{SiO_2}\right)/\left(m_{SiO_2}/\rho_{SiO_2}\right)} - d_{cores} \qquad (4\text{-}1)$$

$$m_{TiO_2} = M_{TiO_2} \cdot C_{TBOT} \cdot V_{Total} \cdot \rho_{TBOT} / M_{TBOT} \qquad (4\text{-}2)$$

3 where m_{SiO2}=0.025g, ρ_{TiO2}=2.9g/cm^3, ρ_{TBOT}=0.996g/cm^3, V_{total}=50ml and ρ_{SiO2}=2.648g/cm^3. As

4 seen in **Figure 5f**, both T and T_{thero} increased with increasing C_{TBOT} in reaction solution, and

5 showed good agreement with each other when C_{TBOT} ≤0.75 vol. %, indicating the high

6 conversion rate of TBOT and the high yield of TiO_2 coating in this method. Particle

7 agglomeration was well prevented in a considerably wide range of C_{TBOT} (0.20 to 0.75 vol. %),

8 indicating the regulation role of acetone remained effective in this range. Especially,

9 monodisperse STcsps with 107nm in their TiO_2 shells could be obtained by controlling C_{TBOT}

10 at 0.75 vol. % (**Figure 5d**). However, T was significantly larger than the corresponding T_{thero}

11 when C_{TBOT} was further increased to 1.00 vol. %. Apparently, the formation of necks (marked

12 in **Figure 5e**) with such a high C_{TBOT} decreased the effective surface area for TiO_2 coating, and

13 thus led to unusually thick TiO_2 shells. In fact, it was hard to construct a thick (~100nm) TiO_2

14 shell on the surface of cores by simply increasing C_{TBOT} in the conventional reaction solution

15 of ethanol/NH_3/TBOT, since a higher C_{TBOT} led a higher hydrolysis rate of TBOT—and thus a

16 higher risk for particle agglomeration. Instead, multiple coating with adopting low C_{TBOT} in

17 every step and/or surfactants-assisted fabrication was usually applied [27, 28]. While in the present

18 experiments, profiting from the regulation role of acetone, the hydrolysis rate of TBOT and the

19 condensation rate of titanium oligomers were able to balance with each other at different C_{TBOT}.

20 Therefore, the thickness of TiO_2 shells became tunable within a considerable wide range by

varying the addition volume of TBOT. Although there still was an upper limit on C_{TBOT} for

maintaining the dispersibility of the resulting core-shell particles, thick TiO_2 shells (e. g. 107nm)

could be constructed on cores evenly in a one-pot synthesis.

3.5 Crystallization of TiO_2 shells

Considering the crystallized TiO_2, especially the anatase TiO_2, is much more desirable than

amorphous one in applications, we investigated the crystallization process of the obtained TiO_2

shells. TG-DTA curves of STcsps (T=85nm) and SiO_2 cores in the temperature range of

$20\sim800^oC$ are compared in **Figure 6a**. As seen, both TG curves kept declining with temperature

increasing until they reached to a platform at around 500^oC. However, due to the new portion

of water and organic residues brought by TiO_2 coating, the total weight loss of STcsps (26%)

was much higher than that of SiO_2 cores (9%). Besides, no peaks could be found in the DTA

curve of SiO_2 cores, whereas there were a number of exothermic peaks appeared in that of

STcsps (300~450°C), which were caused by the combustion of organic residuals. It should be

point out the amount of organic residuals in the obtained STcsps was considerably low, as

revealed by the small difference between TG curves obtained with and without nitrogen

protection (**s5**). Noteworthy, all those exothermic peaks are not about to the crystallization

process, since XRD measurement (**Figure 6b**) indicated the TiO_2 shell were still amorphous

after calcining STcsps in air at 500^oC for 5h. It is found in **Figure 6b** that TiO_2 shell started to

crystallize at around 550^oC, as a small diffraction peak appeared in the corresponding XRD

pattern ($2\theta=25.4^o$). When the calcination temperature was increased to 600^oC, the intensity of

that peak significantly increased, indicating TiO_2 shell increased in its crystallinity. Meanwhile,

more diffraction peaks appeared in the XRD pattern, all of which could be well indexed to the

standard XRD diffraction pattern of anatase TiO_2 (JCPDS No. 21-1272). Normally, the typical calcination temperature for obtaining anatase TiO_2 is 500°C [26], but it was insufficient for the crystallization of TiO_2 shells in this work, suggesting the phase transformation of TiO_2 was possibly inhibited by compositing with SiO_2 cores. Furthermore, the grain size of the formed anatase shells (600°C, 5h) was calculated to 9nm by Scherrer equation. Such a small grain size indicated the high nucleation rate of TiO_2 in the coating process.

On the morphology of STcsps with crystallized TiO2 (anatase) shells, **Figure 6c and 6d** show the low- and high-magnification TEM images of calcined (600°C) STcsps, respectively. As seen, the crystallized TiO_2 shells remained complete and uniform on the surface of SiO_2 cores, no new necks or aggregates formed in calcination. In addition, the anatase type of the crystallized TiO_2 shells could also be confirmed by the lattice fringes shown in the high-magnification TEM image (insert of **Figure 6d**), as the distance between two fringes (0.35nm) was close to the spacing of (101) lattice of anatase TiO_2 (0.3514nm).

4. Conclusion

In summary, we have demonstrated a facile method for constructing uniform TiO_2 shells. Two common issues in the TiO_2 coating by conventional sol-gel method, as one about the uniformity of TiO_2 shells and another one on the dispersibility of core-shell particles, have been successfully addressed. Even more importantly, the TiO_2 coating by this method could reach to a high yield rate within a short time and the corresponding shell thickness could be simply tuned by the usage amount of precursor TBOT. As observed, uniform and complete TiO_2 shells with a tunable thickness from 30 to 107nm could be constructed on SiO_2 cores (366±3nm) in 2h to form $SiO_2@TiO_2$ core-shell particles with high dispersibility. All

advantages of this method could be attributed to the presence of acetone in the reaction

system with an appropriate fraction, as it not only promoted the yielding of TiO_2, but also

regulated the concentration of titania oligomers to a desirable level for the heterogeneous

nucleation of TiO_2. In this method, the presence of NH_3 was also important for the formation

of complete TiO_2 shells, though the concentration of NH_3 had to be controlled at low. In

addition, the obtained TiO_2 shells could be further crystallized to anatase shells by calcining

in air at 600°C, and thus to meet practical applications.

We believe this method can be extended for various core materials, as the formation rate

of TiO_2 could be well controlled by optimizing the fraction of acetone in reaction solution

even without cores (the fabrication of monodisperse TiO_2 microspheres). Moreover, the

success of this method suggests much more attention should be devoted to the solvent effect

in the sol-gel process of ceramic core-shell particles. In the following works, it is also worthy

to comparing the interaction between acetone and titanium oligomers to that between ethanol

and titanium oligomers for better understanding the regulation role of acetone towards TiO_2

coating.

Reference

[1]   Suying Wei, Qiang Wang, Jiahua Zhu   Luyi Sun, Hongfei Line, Zhanhu Guo,

Multifunctional composite core–shell nanoparticles, Nanoscale 3 (2011) 4474-4502.

[2] Hiroaki Tada, Musashi Fujishima, Hisayoshi Kobayashi, Photodeposition of metal sulfide quantum dots on titanium (IV) dioxide and the applications to solar energy conversion, Chem. Soc. Rev. 40 (2011) 4232-4243.

[3] Jifa Qi, Xiangnan Dang, Paula T. Hammond, Angela M. Belcher, Highly efficient plasmon-enhanced dye-sensitized solar cells through metal@oxide core–shell nanostructure, ACS Nano 5 (2011) 7108–7116.

[4] Jiang Du, Jian Qi, Dan Wang, Zhiyong Tang, Facile synthesis of Au@TiO2 core–shell hollow spheres for dye-sensitized solar cells with remarkably improved efficiency, Energy Environ. Sci. 5 (2012) 6914-6918.

[5] Suim Son, Sun Hye Hwang, Chanhoi Kim, Ju Young Yun, Jyongsik Jang, Designed synthesis of SiO_2/TiO_2 core/shell structure as light scattering material for highly efficient dye-sensitized solar cells, ACS Appl. Mater. Interfaces 5 (2013) 4815-4820.

[6] Jianping Ge, Qiao Zhang, Tierui Zhang, Yadong Yin, Core–Satellite nanocomposite catalysts protected by a porous silica shell: controllable reactivity, high stability, and magnetic recyclability, Angew. Chem., Int. Ed. 47 (2008) 8924-8928.

[7] F H Chen, Q Gao, J Z Ni, The grafting and release behavior of doxorubincin from $Fe_3O_4@SiO_2$ core–shell structure nanoparticles via an acid cleaving amide bond: the potential for magnetic targeting drug delivery, Nanotechnol. 19 (2008) 165103-165112.

[8] I. I. Slowing, B. G. Trewyn, S. Giri, V. S.-Y. Lin, Mesoporous silica nanoparticles for drug delivery and biosensing applications, Adv. Funct. Mater. 17 (2007) 1225-1236.

[9]   Wolfgang Schärtl, Current directions in core–shell nanoparticle design, Nanoscale 2 (2010) 829-843.

[10] Jing Yuan, Zhenguo An, Bing Li, Jingjie Zhang, Facile aqueous synthesis and thermal insulating properties of low-density glass/TiO_2 core/shell composite hollow spheres, Particuology 10 (2012) 475-479.

[11] Vladimir V. Srdić, Bojana Mojić, Milan Nikolić, Stevan Ognjanović, Recent progress on synthesis of ceramics core/shell nanostructures, Process. Appl. Ceramics 7 (2013) 45-62.

[12] Yao Qin, Yanjie Zhou, Jie Li, Jie Ma, Donglu Shi, Junhong Chen, Jinhu Yang, Fabrication of hierarchical core–shell Au@ZnO heteroarchitectures initiated by heteroseed assembly for photocatalytic applications, J. Colloid Interface Sci. 418 (2014) 171-177.

[13] Li Zhang, Douglas A. Blom, Hui Wang, Au–Cu_2O core–shell nanoparticles: a hybrid metal-semiconductor heteronanostructure with geometrically tunable optical properties, Chem. Mater., 23 (2011) 4587-4598.

[14] Yong Wang, Xiaowen S , Panshuang Ding, Shan L , Huaping Yu, Shape-controlled synthesis of hollow silica colloids, Langmuir 29 (2013) 11575-11581.

[15] Tian-Song Deng, Frank Marlow, Synthesis of monodisperse polystyrene@vinyl-SiO_2 core–shell particles and hollow SiO_2 spheres, Chem. Mater. 24 (2012) 536-542.

[16] C. Karunakaran, P. Vinayagamoorthy, J. Jayabharathi, Electrical, optical and photocatalytic properties of polyethylene glycol-assisted sol–gel synthesized Mn-doped TiO_2/ZnO core–shell nanoparticles, Superlattices Microstruct. 64, (2013) 569-

580.

[17] Jong Min Kim, Sang Mok Chang, Sungkook Kim, Kyo-Seon Kim, Jinsoo Kim, Woo-Sik Kim, Design of SiO_2/ZrO_2 core–shell particles using the sol–gel process, Ceram. Int. 35 (2009) 1243-1247.

[18] F. Caruso, Nanoengineering of particle surfaces, Adv. Mater. 13 (2001) 11-22.

[19] Hui Liu, , Tingting Liu, Xiaonan Dong, Rui Hua, Zhenfeng Zhu, Preparation and enhanced photocatalytic activity of Ag-nanowires@SnO_2 core–shell heterogeneous structures, Ceram. Int. 40 (2014) 16671-16675.

[20] Guozhi Zhang, Feng Teng, Changhui Zhao, Lulu Chen, Peng Zhang, Youqing Wang, Chengshi Gong, Zhenxing Zhang, , Erqing Xie, Enhanced photocatalytic activity of TiO_2/carbon@TiO_2 core–shell nanocomposite prepared by two-step hydrothermal method, Appl. Surf. Sci. 311 (2014) 384-390.

[21] Christina Graf, Dirk L. J. Vossen, Arnout Imhof, Alfons van Blaaderen, A general method to coat colloidal particles with silica, Langmuir 19 (2003) 6693–6700.

[22] Wei Li, Jianping Yang, Zhangxiong Wu, Jinxiu Wang, Bin Li, Shanshan Feng, Yonghui Deng, Fan Zhang, Dongyuan Zhao, A versatile kinetics-controlled coating method to construct uniform porous TiO_2 shells for multifunctional core–shell structures, J. Am. Chem. Soc. 134 (2012) 11864-11867.

[23] Werner Stöber, Arthur Fink. Controlled growth of monodisperse silica spheres in the micron size range, J. Colloid Interface Sci. 26 (1968) 62-69.

[24] Morten E. Simonsen, Erik G. Søgaard, Sol–gel reactions of titanium alkoxides and water: influence of pH and alkoxy group on cluster formation and properties of the

resulting products, J. Sol-Gel Sci. Technol. 53 (2010) 485-497.

[25]   Victor K. LaMer , Robert H. Dinegar, Theory, production and mechanism of formation of monodispersed hydrosols, J. Am. Chem. Soc. 72 (1950) 4847-4854.

[26]   Xuchuan Jiang, Thurston Herricks, Younan Xia, Monodisperse spherical colloids of titania: synthesis, characterization, and crystallization, Adv. Mater. 15 (2003) 1205-1209.

[27]   J.W. Lee, M.R. Othman, Y. Eomc, T.G. Lee, W.S. Kim, J. Kim, The effects of sonification and TiO_2 deposition on the micro-characteristics of the thermally treated SiO_2/TiO_2 spherical core–shell particles for photo-catalysis of methyl orange, Micropor Mesopor Mater. 116 (2008) 561-568.

[28]   Ji Bong Joo, Qiao Zhang, Ilkeun Lee, Michael Dahl, Francisco Zaera, Yadong Yin, Mesoporous anatase titania hollow nanostructures though silica-protected calcination, Adv. Funct. Mater. 22 (2012) 166-174.

1

2

3

4

5

6

7

8

9

10

Table 1 Recipes for the fabrication of STcsps .

No.	$R_{a/e}^{1, 2}$	$V_{28\% \text{ ammonia}}$/ml	C_{TBOT}/vol.%	Dispersibility	d^4/nm
1	0	0.15	0.60	Good	366±3
2	0.4	0.15	0.60	Good	366±3
3	0.8	0.15	0.60	Good	392±14
4	1.2	0.15	0.60	Good	536±5
5	1.6	0.15	0.60	Necks	NA^5
6	2.0	0.15	0.60	Agglomeration	NA
7	1.2	0^6	0.60	Necks	NA
8	1.2	0.25	0.60	Agglomeration	NA
9	1.2	0.15	0.20	Good	426±5
10	1.2	0.15	0.30	Good	466±4
11	1.2	0.15	0.45	Good	510±8
12	1.2	0.15	0.75	Good	580±6
13	1.2	0.15	1.00	Necks	692±9

[1] the volume ratio of acetone to ethanol; [2] total volume=50ml; [3] mean size of resulting particles, calculated by evaluating100 particles in SEM image; [4] not applicable due to particle agglomeration; [6] replacing 0.15ml 28% ammonia solution with 0.11ml DI water.

1

2

3

4
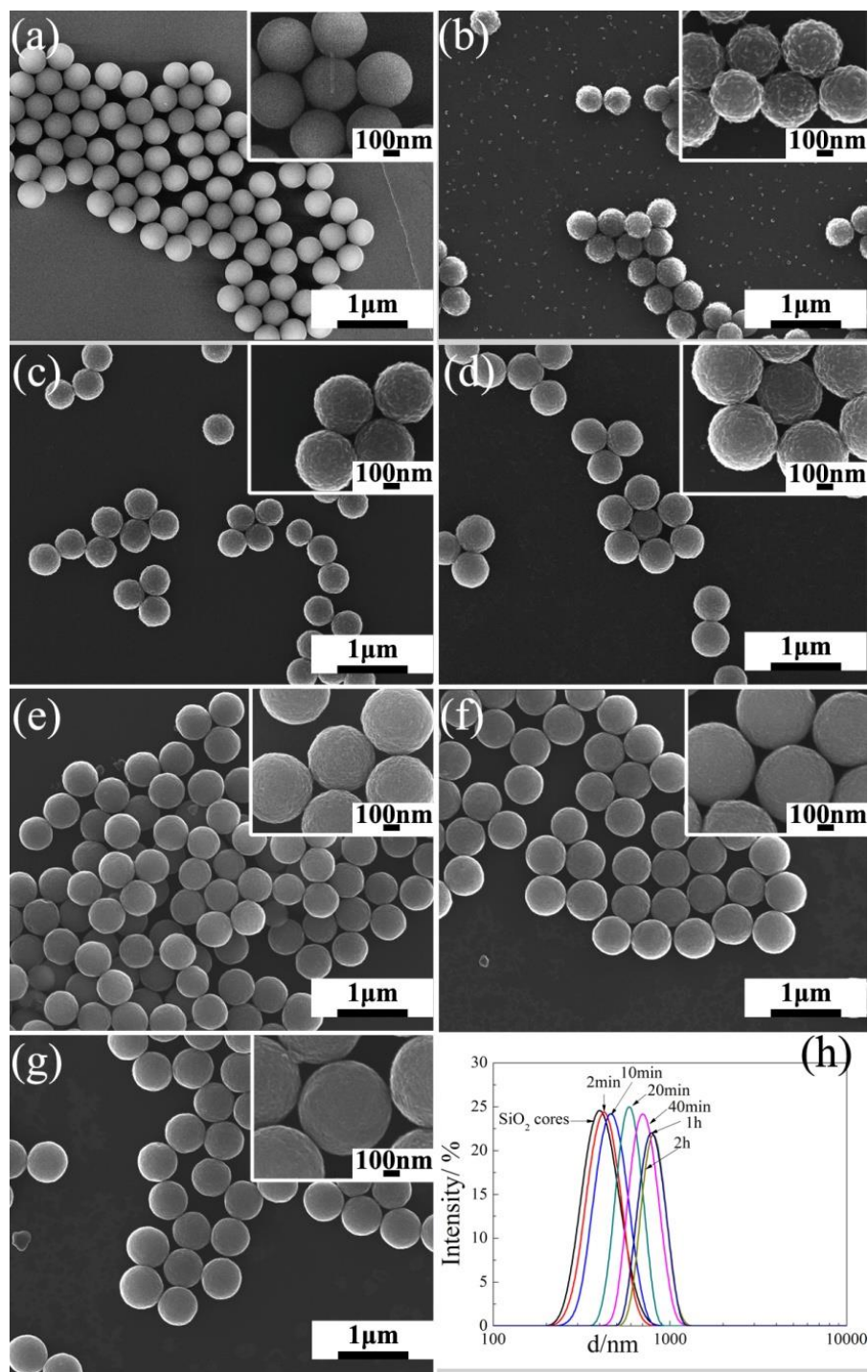
Figure 1. SEM images of SiO$_2$ cores (a) and intermediate productions of STcsps after TiO$_2$ coating for 2min (b), 10min (c), 20min (d), 40min (e), 60min (f), and 120min (g); (h) shows the corresponding size distribution curves obtained from DLS measurements; in this synthesis, R$_{a/e}$, addition volume of ammonia solution and C$_{TBOT}$ were controlled at 1.2, 0.15ml and 0.6 vol.% respectively (**recipe 4**).

22
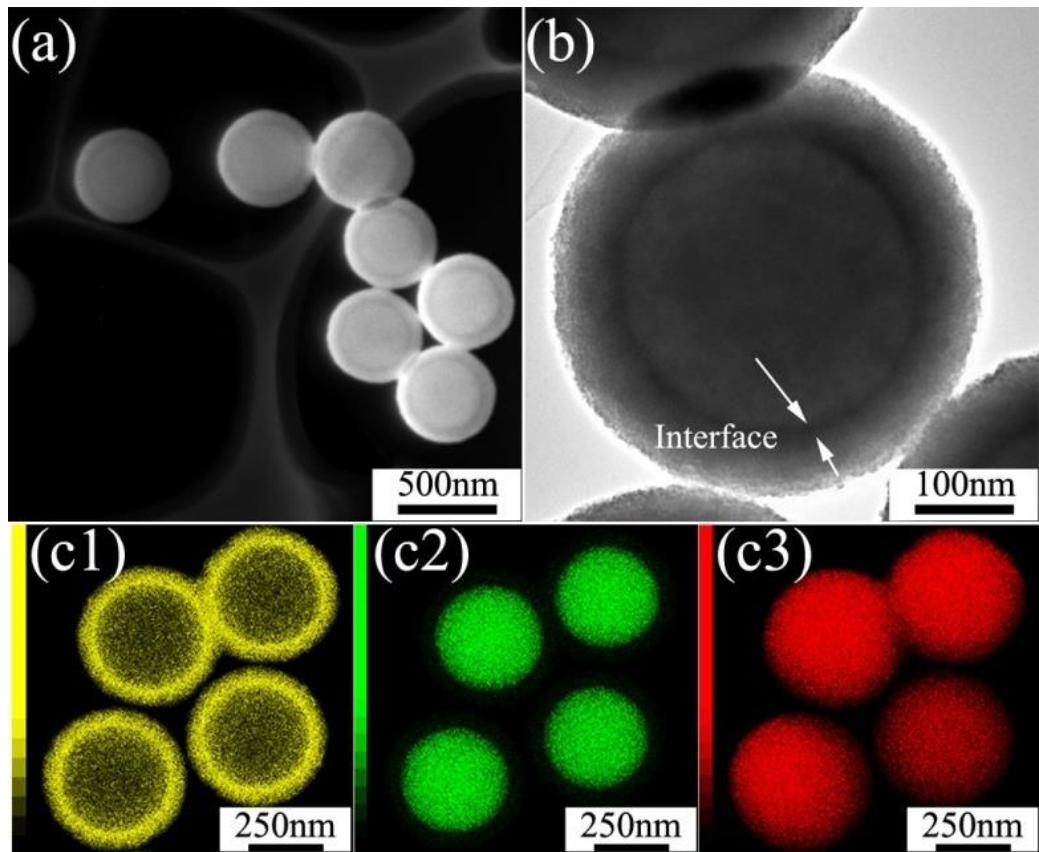
Figure 2. (a) dark field TEM image of the as-fabricated STcsps; (b) high-magnification TEM image of STcsps; (c) EDS mappings demonstrating the distribution of element Ti (c1), Si (c2) and O (c3) in STcsps.

1

2
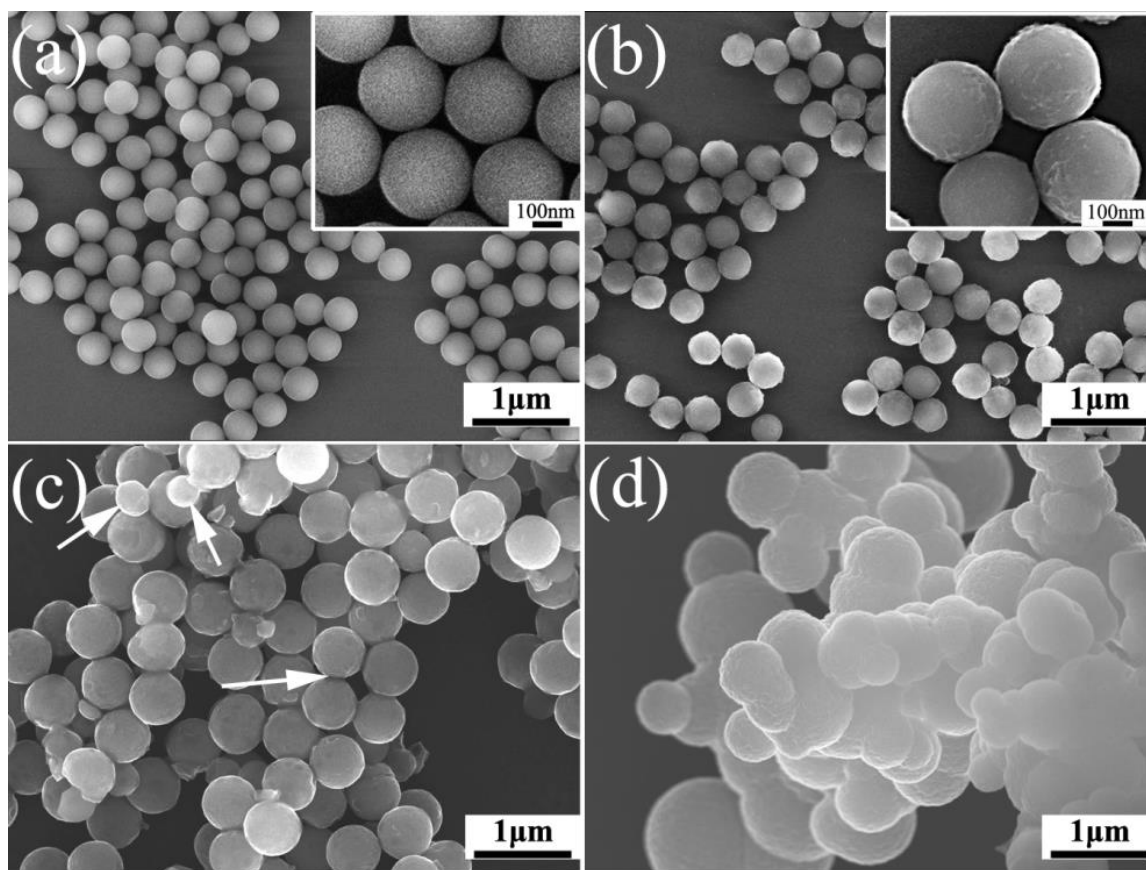
Figure 3. SEM images of STcsps formed in the reaction solution with $R_{a/e}$ equal to 0.4 (a), 0.8

(b), 1.6 (c) and 2.0 (d); arrows in (c) point to freestanding TiO_2 particles and/or necks.

5

6

7

8

9

10

11

12

13

1

2
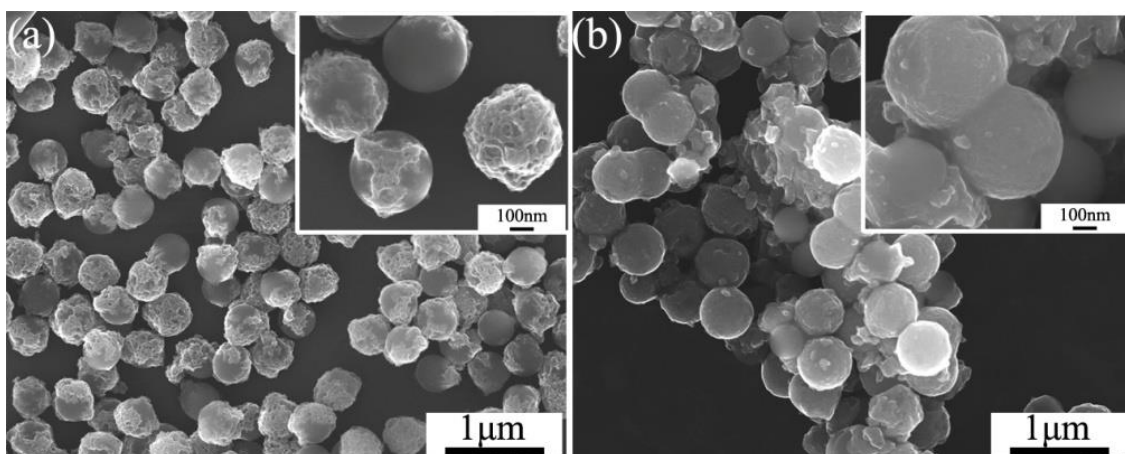
Figure 4. SEM image of (a) SiO_2/TiO_2 composite particles formed fabricated without the

presence of NH_3 (**recipe 7**), (b) STcsps fabricated with adding 0.25ml 28% ammonia solution

into the reaction solution.

6

7

8

9

10

11

12

13

14

15

16

17

18

1

2
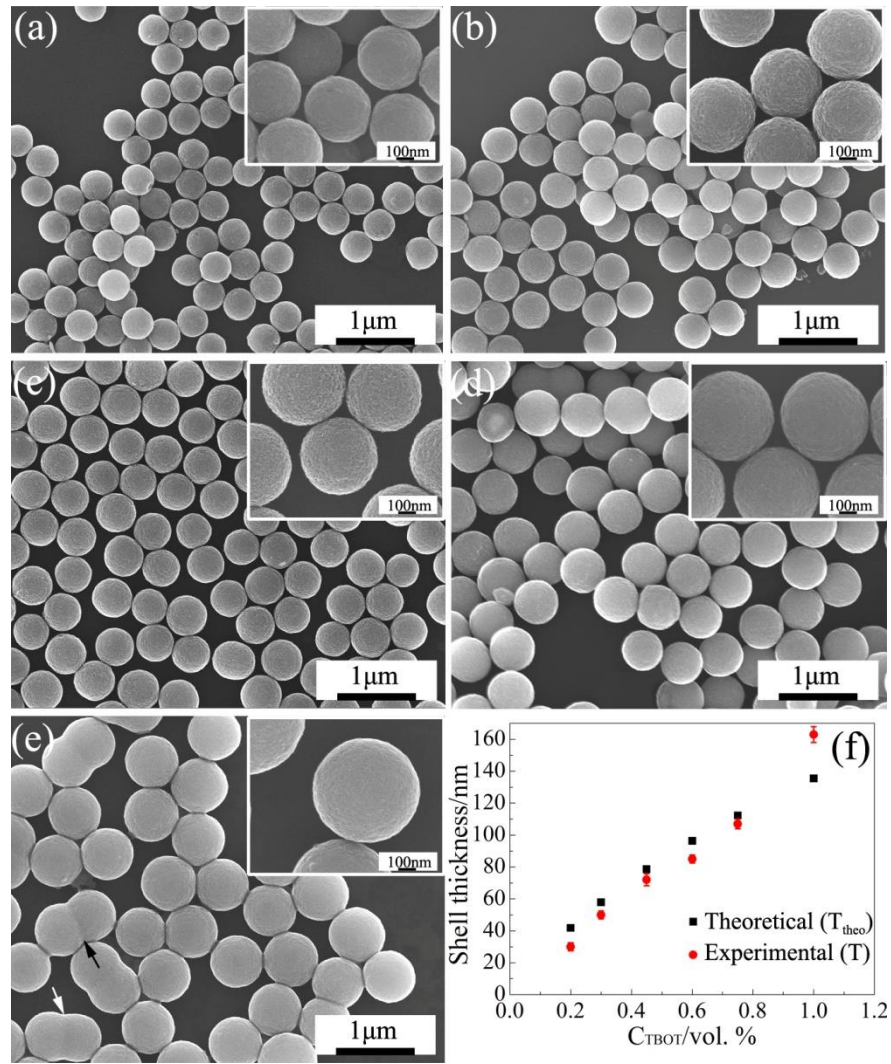
Figure 5. SEM images of STcsps fabricated with controlling C_{TBOT} at 0.20 vol. % (a), 0.30

vol. % (b), 0.45 vol. % (c), 0.75 vol. % (d), and 1.00 vol. % (e); (f) plots both TiO_2 shell

thickness (T) and corresponding theoretical thickness (T_{theo}) as functions of C_{TBOT}.

6

7

8

9

10

11

1

2
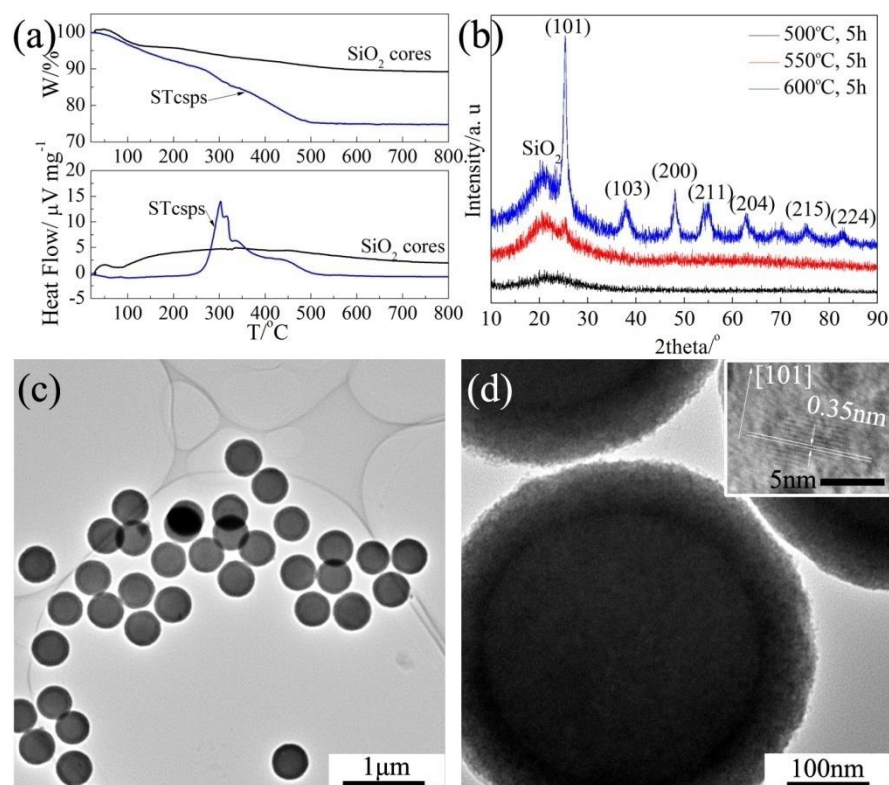
3 **Figure 6.** (a)TG-DTA curves of STcsps and SiO$_2$ cores under air flow with the sweeping

4 rate of 10$^{\rm o}$C/min; (b) XRD patterns of STcsps after being calcined in air at different

5 temperature for 5h; low- (c) and high-magnification (d) TEM images of STcsps after being

6 calcined in air at 600$^{\rm o}$C for 5h.

7

8

9

10

11

12

13

14

Supplementary Materials

A Modified Sol-Gel Method for Fast Constructing Uniform TiO$_2$ Shells with Tunable Thickness to Fabricate Monodisperse SiO$_2$@TiO$_2$ Core-Shell Particles

Author name: Wanghui Chen, Chika Takai, Hadi Razavi Khosroshahi, Masayoshi Fuji*, Takashi Shirai

Author affiliation: Advanced Ceramics Research Center, Nagoya Institute of Technology, Honmachi 3-101-1, Tajimi, Gifu, 507-0033, Japan
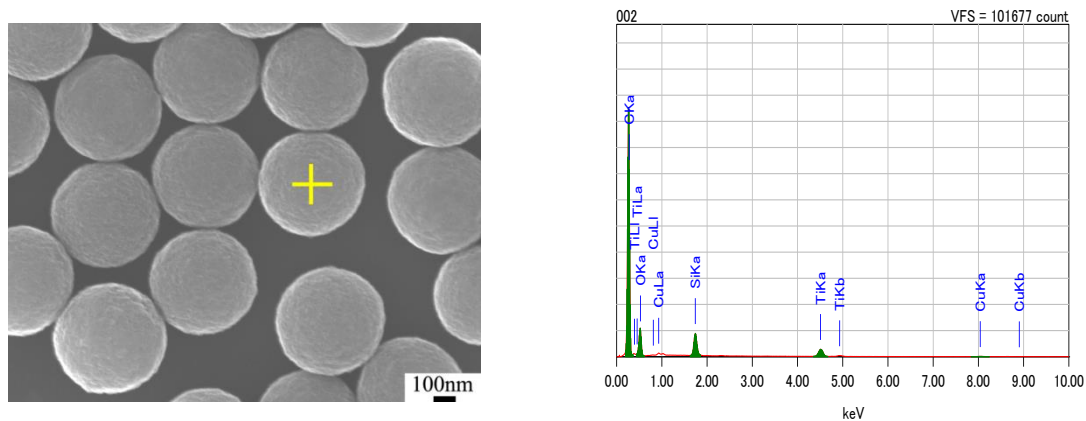
*Corresponding author: E-mail: fuji@nitech.ac.jp; Tel.: +81 572 24 8110; Fax: +81 572 24 8109.

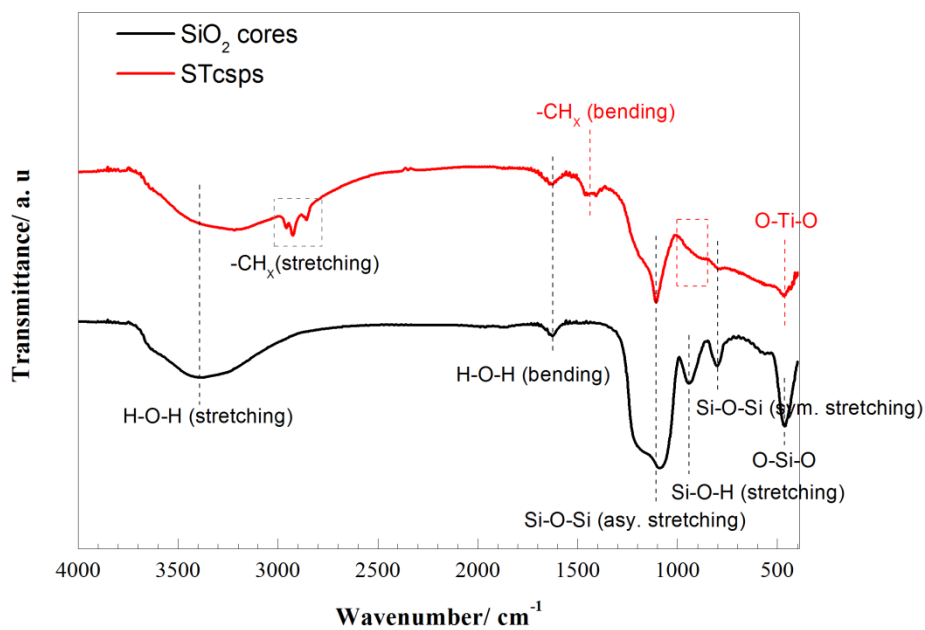**Figure S1.** EDS point spectra of SiO$_2$ cores.
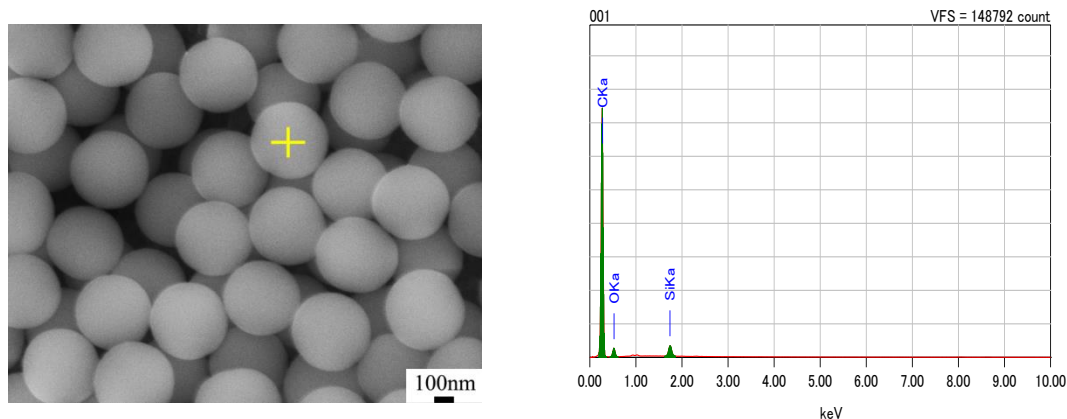
1
2
3
4
5

Figure S2. EDS point spectra of STcsps.
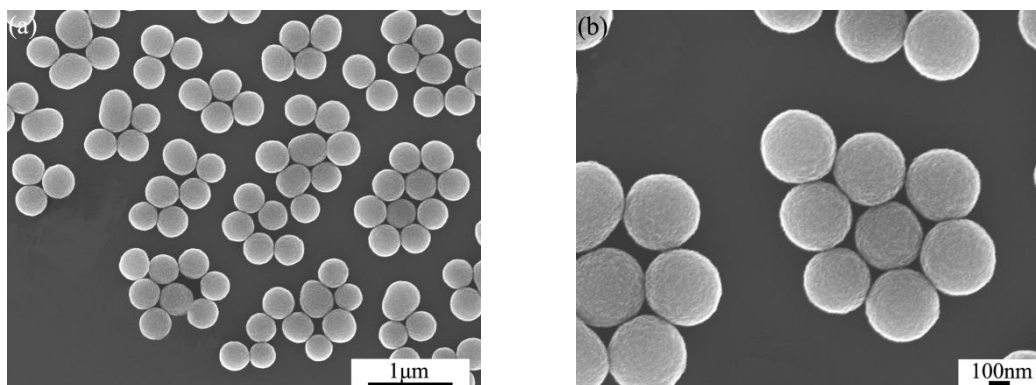

6
7
8
9
10
11
12
13

Figure S3. FT-IR spectra of SiO$_2$ cores and STcsps.

* The decreasing on the intensity of the peak for Si-O-H stretching indicates most

isolated silanols on the surface of SiO_2 cores were replaced by Si-O-Ti after TiO_2 coating.

1

2

3

Figure S4. low- (a) and high-magnification (b) SEM of obtained monodisperse TiO2 microspheres.

Recipe: $R_{a/e}$=1.5; total volume=50ml; C_{TBOT}=0.5vol. %; $V_{28\% \ ammonia \ solution}$=0.15ml; time reaction=2h

4

5

6

7

8

Figure S5. TG-DTA curves of STcsps (T=85nm) with and without the protection of N_2; heating rate: 5°C/min.

1